

Supplemental information for:

Rh-Promoted Mixed Oxides for “Low-Temperature” Methane Partial Oxidation in Absences of Gaseous Oxidants

This section includes detailed information about the experiments and characterizations performed in this study.

Pulse injection panel

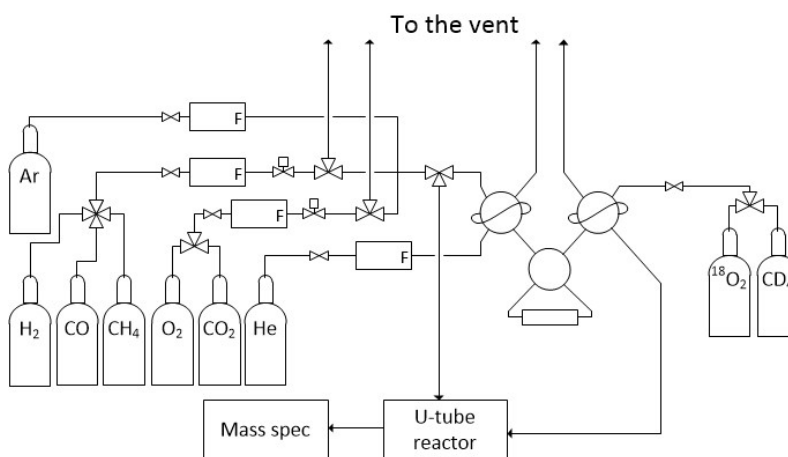


Figure S1. Schematic of pulse injection panel set-up

X-ray diffraction experiments and Rietveld refinement analysis

Powder X-ray diffraction experiments were done to confirm the formation of the desired crystal phases. XRD patterns were obtained using a Rigaku SmartLab X-ray diffractometer with Cu-K α ($\lambda=0.1542$) radiation operating at 40 kV and 44 mA. A stepwise approach with a step size of 0.1° and residence time of 2.5 seconds at each step in $20-80^\circ$ angle range (2θ) was used to generate the XRD patterns. Figure S2 shows the XRD patterns of the as prepared samples. It is obvious that the position and intensity of the peaks match the reference peaks of cubic fluorite LaCeO_{3.5} and orthorhombic perovskite CaMnO₃ pretty well. No apparent change in XRD patterns is observed after addition of Rh. Similar experiments were also performed on the spent samples to confirm their phase stability. Figure S3 shows the XRD pattern of the Rh-promoted CaMnO₃ after 5 redox cycles at 900 °C and 10% CH₄/O₂. As can be seen, no major structural change was observed on the sample after redox cycles.

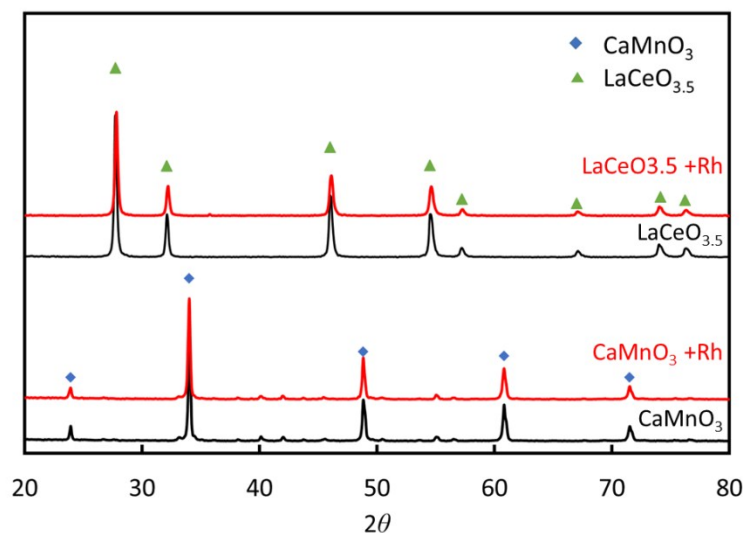


Figure S2. XRD patterns of as prepared unpromoted and Rh-promoted CaMnO₃ and LaCeO_{3.5}

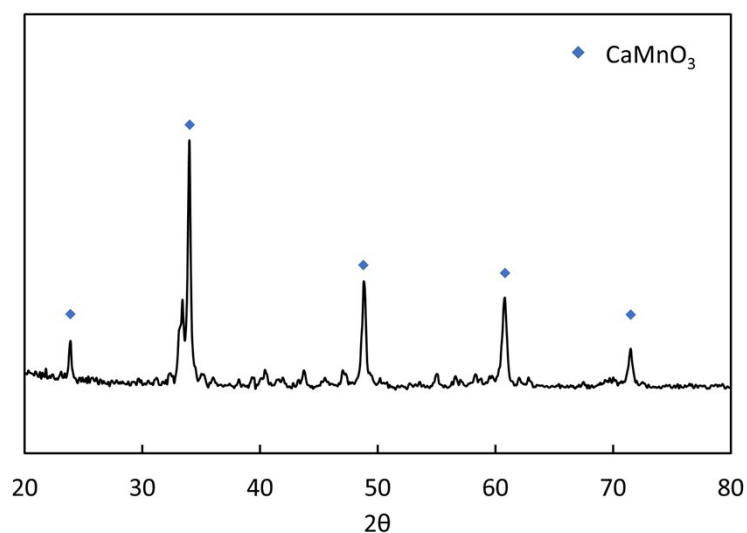


Figure S3. XRD pattern of Rh-promoted CaMnO₃ after 5 redox cycles at 900 °C and 10 Vol. % CH₄/O₂

Rietveld refinement is used to analyze the effects of Rh addition on the crystal structure of the base mixed oxides more closely. XRD patterns are collected on a high resolution Empyrean PANalytical XRD instrument using a similar Cu K α radiation operating at 45 kV and 40 mA. A stepwise scan is used (2 θ range of 20–80) with a step size of 0.01° holding each step for 200 s. Table S1 summarizes the Rietveld refinement data on CaMnO₃ after addition of Rh. Results confirmed very minimal change in the lattice parameters, which indicates minimal incorporation of Rh in the CaMnO₃ lattice. Refinement analysis was not done on the LaCeO₃-based samples as very high purity phases and immaculate XRD patterns are needed and for reliable refinement analysis which are not observed on the LaCeO₃-based samples.

Table S1. Rietveld refinement analysis data for CaMnO_3 (Orthorhombic, Pbcm) after addition of 0.5 wt% Rh which corresponds to 0.7% Rh in the B-site of the perovskite structure

Parameter	CaMnO_3	CaMnO_3+Rh
a (Å)	5.281	5.281
b (Å)	7.455	7.456
c (Å)	5.267	5.272

Temperature programmed reduction (TPR) experiments

Methane TPR experiments are performed in 10% methane (balance Ar) and temperature ramping rate of 20 °C/min. Figure S4 shows the weight loss percent of the un-promoted and promoted redox catalysts during the methane TPR experiments. It is apparent that addition of Rh-promoter significantly reduced (by almost 200 °C) the onset of reduction of both redox catalysts.

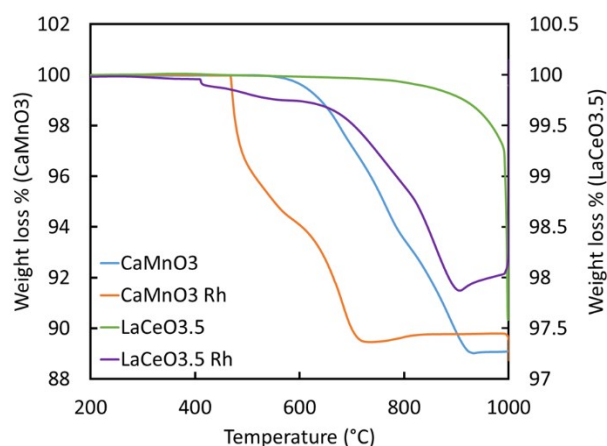


Figure S4. Comparison of the weight loss of the redox catalysts during methane TPR experiments

Methane redox experiments at 900 °C

Methane redox experiments are performed in a U-tube quartz reactor with 50 mg redox catalyst loading. Figure S5 demonstrates the product distribution pattern of the un-promoted and promoted redox catalysts at 900 °C. Both samples kinetic and selectivity enhancements after addition of the Rh promoter. The kinetic effect is much more obvious as the reaction time is reduced by more than 10 times. CaMnO_3 experienced a less significant kinetic improvement as it is already pretty active at this temperature. However, increase in CO formation kinetics is obvious.

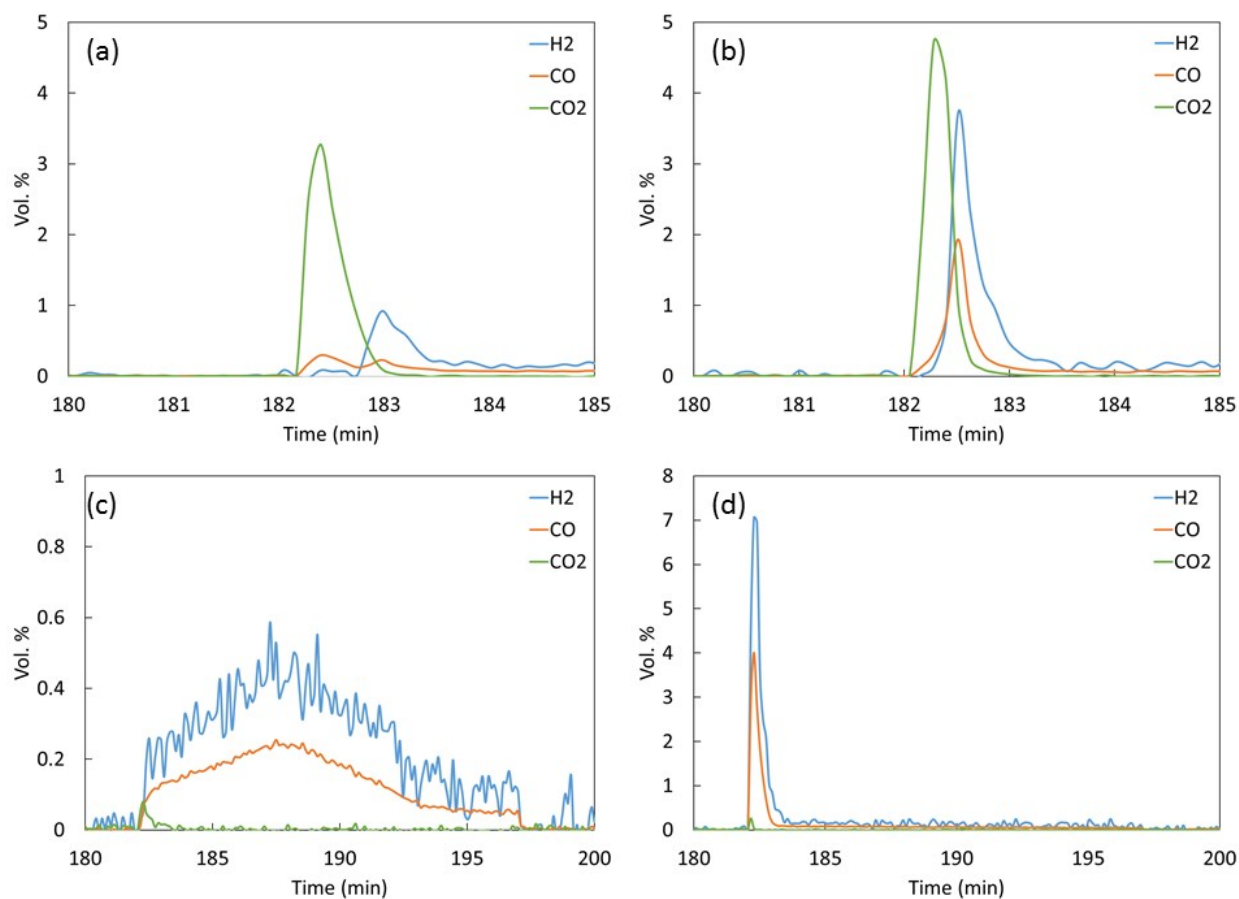


Figure S5. Product distribution during methane reduction half cycle at 900 °C and 10% methane using (a) CaMnO_3 , (b) $\text{CaMnO}_3+0.5\% \text{ Rh}$, (c) $\text{LaCeO}_{3.5}$, and (d) $\text{LaCeO}_{3.5}+0.5\% \text{ Rh}$

Methane conversion in the presence of gaseous oxygen

To determine the effect of Rh on surface methane activation, methane-oxygen cofeed experiments are conducted. Five oxygen to methane ratios were used (O_2/CH_4 : 1.5, 1, 0.5, 0.2, and 0.1). The selectivities, methane and oxygen conversions, and CO yields are compared in Figures 4, S6, S7, and S8.

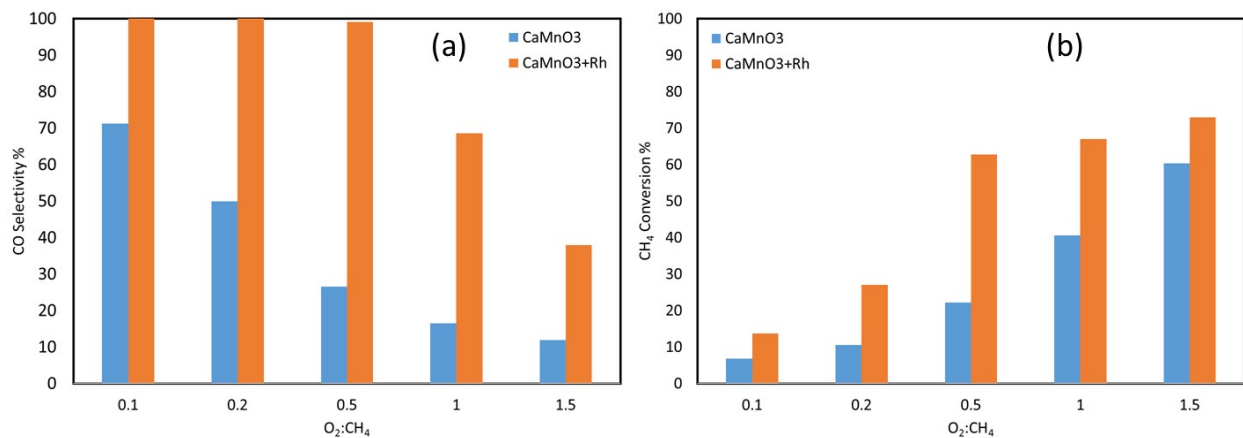


Figure S6. Comparison of (a) CO selectivity and (b) methane conversion during methane-oxygen cofeed experiments using un-promoted and Rh-promoted CaMnO₃-based redox catalyst

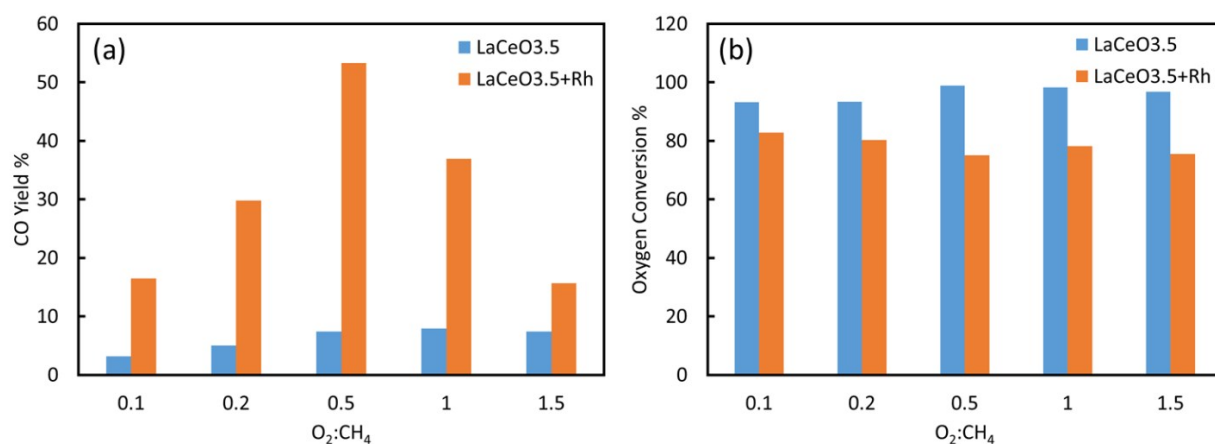


Figure S7. Comparison of (a) CO Yield and (b) oxygen conversion during methane-oxygen cofeed experiments using un-promoted and Rh-promoted LaCeO_{3.5}-based redox catalyst

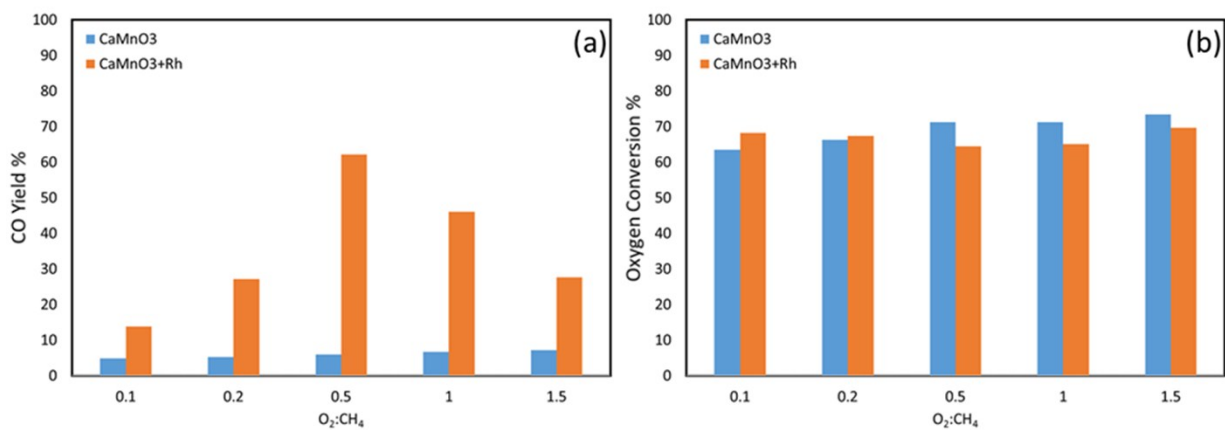


Figure S8. Comparison of (a) CO Yield and (b) oxygen conversion during methane-oxygen cofeed experiments using un-promoted and Rh-promoted CaMnO₃-based redox catalyst

CO desorption DRIFTS Experiments

DRIFTS experiments are performed on $\text{LaCeO}_{3.5}$ -based samples to investigate the effect of Rh promoter in bond activation. Carbon monoxide is used as the probe molecule. It is evident that the two surfaces demonstrate different CO surface species. While un-promoted samples only formed carbonate species ($1300\text{-}1600\text{ cm}^{-1}$), the presence of Rh gives rise to carbonyl group formation ($1980\text{-}2110\text{ cm}^{-1}$). Both of these activated species are desorbed or converted to CO_2 at higher temperatures.

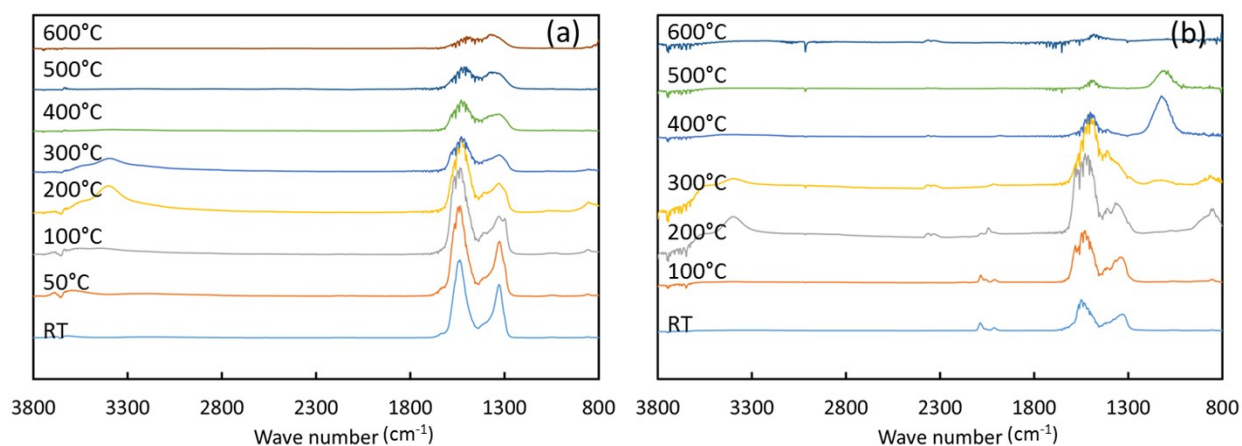


Figure S9. DRIFTS spectra of the CO adsorption/desorption experiments on (a) un-promoted and (b) Rh-promoted $\text{LaCeO}_{3.5}$ sample

Low temperature Redox experiments

Redox experiments similar to those presented in the paper are performed at lower temperatures to investigate the effect of temperature on redox behavior of the redox catalysts. While lowering the temperature to below 800 and $700\text{ }^\circ\text{C}$ significantly suppressed the redox performance of the un-promoted CaMnO_3 (Figure S10) and $\text{LaCeO}_{3.5}$, addition of the Rh promoter kept the samples active at even lower temperatures (Figure S11, Figure S12, Figure S13). Promoted $\text{LaCeO}_{3.5}$ experienced a higher initial oxygen release rate at $600\text{ }^\circ\text{C}$ compared to the un-promoted samples at $900\text{ }^\circ\text{C}$. Selectivity of the promoted CaMnO_3 significantly increased at lower temperatures and maximum CO yield is observed at $600\text{ }^\circ\text{C}$. Table S4 summarizes the maximum oxygen donation and methane conversion rates for these experiments on CaMnO_3 -based redox catalysts. These values are used to calculate the apparent activation energies of the redox reactions.

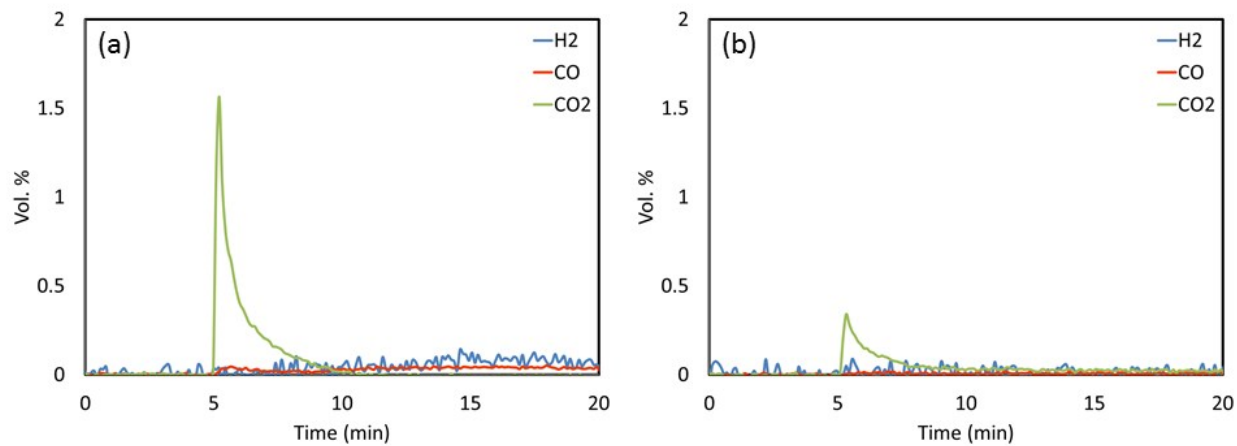


Figure S10. Product distribution during methane reduction half cycle in 10% methane at (a) 800 °C and (b) 700 °C using CaMnO₃

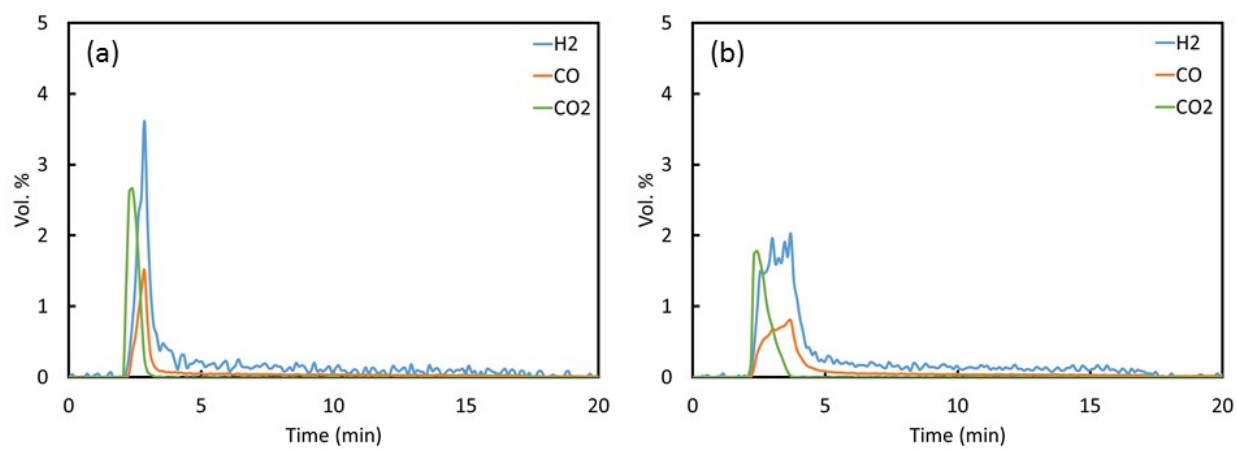


Figure S11. Product distribution during methane reduction half cycle in 10% methane at (a) 800 °C and (b) 700 °C using CaMnO₃+0.5% Rh

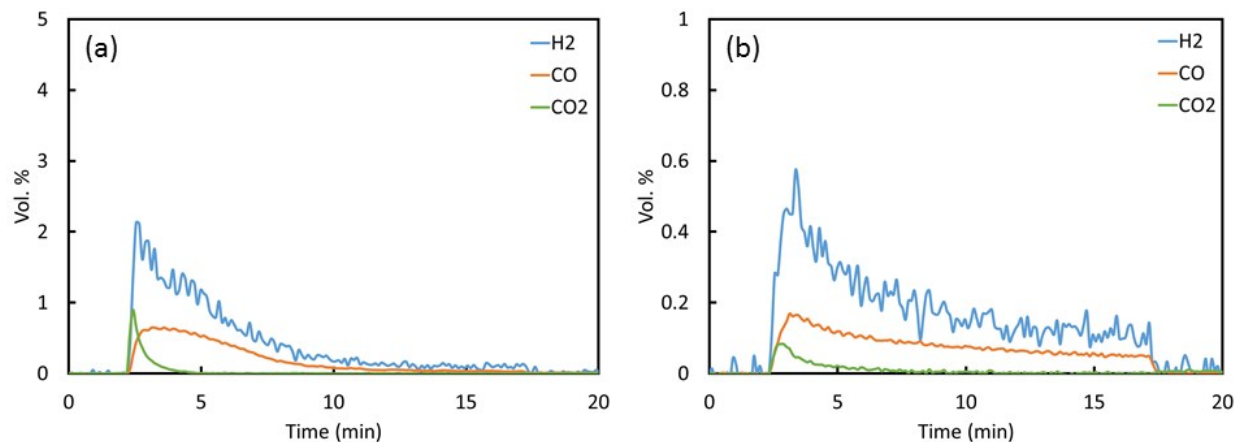


Figure S12. Product distribution during methane reduction half cycle in 10% methane at (a) 600 °C and (b) 500 °C using CaMnO₃+0.5% Rh

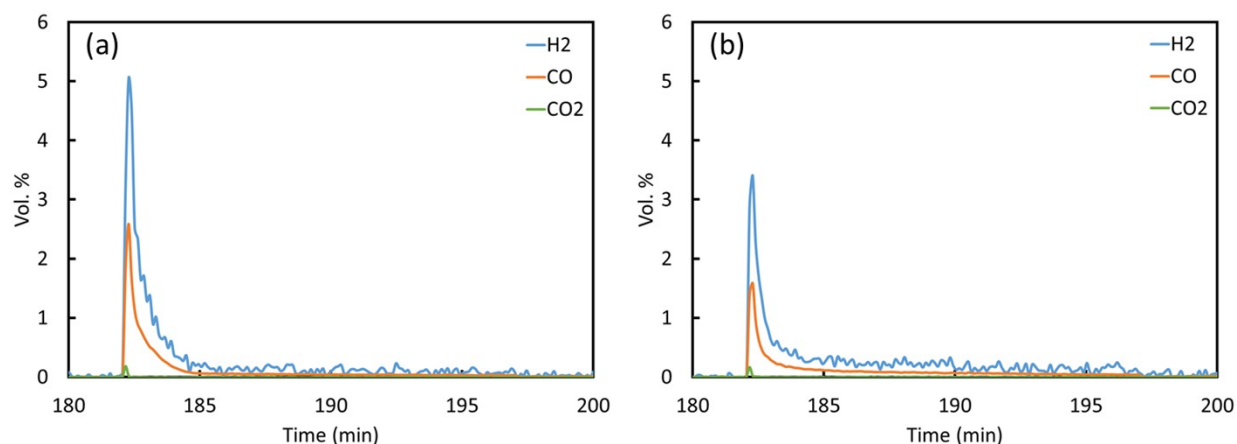


Figure S13. Product distribution during methane reduction half cycle in 10% methane at (a) 800 °C and (b) 700 °C using LaCeO_{3.5}+0.5% Rh

Table S2. Maximum rate of methane conversion and oxygen removal from the CaMnO₃-based redox catalyst in the reduction half-cycle at various temperatures

Redox catalyst	Temperature (°C)	Maximum O ²⁻ removal rate (μmol/s)	Maximum methane conversion rate (μmol/s)
Rh-promoted	900	14.05	3.54
	800	8.18	2.25
	700	5.35	1.57
	600	2.24	0.87
	500	0.25	0.18
Unpromoted	900	9.86	2.50
	800	4.67	1.18
	700	0.98	0.26

Low temperature pulse experiments

To compare the apparent activation energies for oxygen removal and methane conversion on the surface and bulk of the catalyst, methane pulse injection experiments were performed on the CaMnO₃-based redox catalysts at lower temperatures. Results are summarized in Table S4. Since unpromoted samples did not show noticeable activity at temperatures lower than 700 °C, the results are not presented here. These results are used to calculate the apparent activation energies of the surface reactions by fitting an Arrhenius equation. We note that at temperatures above 800 °C, methane reaction with unpromoted CaMnO₃ are limited by methane supply and/or external mass transfer. Therefore, the activation energy for unpromoted CaMnO₃ was determined using the data from 700 and 800 °C.

Table S3. Total methane converted and oxygen atoms removed from the CaMnO₃-based redox catalyst in the first methane pulse injection at various temperatures

Redox catalyst	Temperature (°C)	Maximum O ² -removal rate (μmol)	Maximum methane conversion rate (μmol)
Rh-promoted	900	47.58	24.62
	800	15.73	8.05
	700	4.14	2.37
Unpromoted	900	80.28	40.20
	800	80.50	40.69
	700	76.41	38.46

Effect of methane concentration

Redox experiments at different methane concentrations are performed on the Rh-promoted CaMnO₃ sample to see the effect of methane concentration on selectivity, methane conversion, and coke formation at 600 °C. The overall space velocity is remained constant in all experiment. Results are summarized in Table S2. As can be seen higher methane concentration contributes to better CO/syngas selectivity. This leads to higher overall methane conversion at lower oxygen donations. Instantaneous methane conversion, however, is reduced in higher methane concentrations as expected (Figure S14).

Table S4. Methane conversion, CO/syngas selectivity, oxygen donation, methane conversion, and coke formation of the Rh-promoted CaMnO₃ redox catalysts during the reduction half cycle at 600 °C

CH ₄ concentration	CO selectivity	Syngas Selectivity	methane Converted (mL)	O ₂ extraction (wt. %)	Coke formation (%)
5%	47.97	64.88	24.04	7.71	0.05
10%	65.63	77.62	26.02	6.79	0.06
20%	88.91	96.41	36.69	6.33	0.12

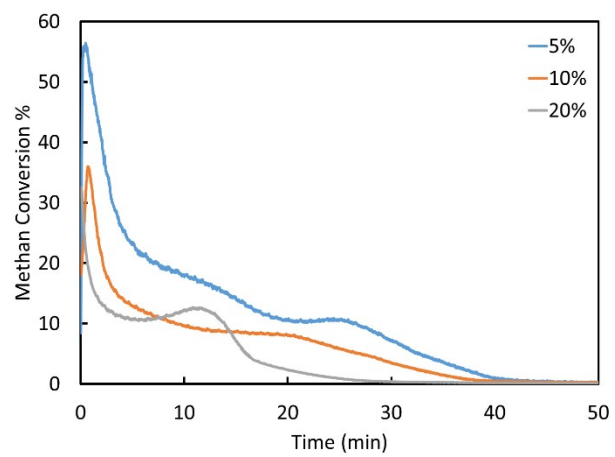


Figure S14. Instantaneous methane conversion on Rh-promoted CaMnO_3 samples during the reduction half-cycle at different methane concentrations